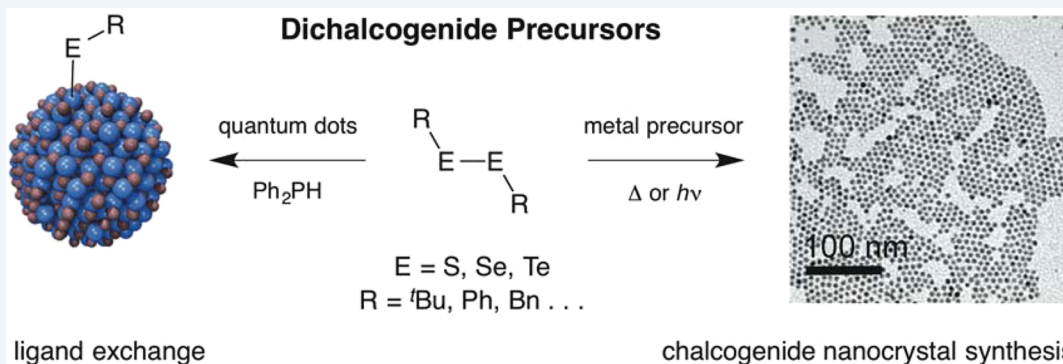


Diorganyl Dichalcogenides as Useful Synths for Colloidal Semiconductor Nanocrystals

Richard L. Brutchey*

Department of Chemistry, University of Southern California, Los Angeles, California 90089, United States



CONSPECTUS: The ability to synthesize colloidal semiconductor nanocrystals in a well-controlled manner (i.e., with fine control over size, shape, size dispersion, and composition) has been mastered over the past 15 years. Much of this success stems from careful studies of precursor conversion and nanocrystal growth with respect to phosphine chalcogenide precursors for the synthesis of metal chalcogenide nanocrystals. Despite the high level of success that has been achieved with phosphine chalcogenides, there has been a longstanding interest in exploring alternate chalcogenide precursors because of issues associated with phosphine chalcogenide cost, purity, toxicity, etc. This has resulted in a large body of literature on the use of sulfur and selenium dissolved in octadecene or amines, thio- and selenoureas, and silyl chalcogenides as alternate chalcogenide precursors for metal chalcogenide nanocrystal synthesis.

In this Account, emerging work on the use of diorganyl dichalcogenides ($R-E-E-R$, where $E = S$, Se , or Te and R = alkyl, allyl, benzyl, or aryl) as alternate chalcogenide precursors for the synthesis of metal chalcogenide nanocrystals is summarized. Among the benefits of these dichalcogenide synthons are the following: (i) they represent the first and only common precursor type that can function as chalcogen transfer reagents for each of the group VI elements (i.e., to make metal oxide, metal sulfide, metal selenide, and metal telluride nanocrystals); (ii) they possess relatively weak $E-E$ bonds that can be readily cleaved under mild thermolytic or photolytic conditions; and (iii) the organic substituents can be tuned to affect the reactivity. These combined attributes have allowed dichalcogenide precursors to be employed for a wide range of metal chalcogenide nanocrystal syntheses, including those for In_2S_3 , $Sn_xGe_{1-x}Se$, $SnTe$, $Cu_{2-x}S_ySe_{1-y}$, $ZnSe$, CdS , $CdSe$, $MoSe_2$, WSe_2 , $BiSe$, and $CuFeS_2$. Interestingly, a number of metastable phases of compositionally complex semiconductors can be kinetically accessed through syntheses utilizing dichalcogenide precursors, likely as a result of their ability to convert at relatively low temperatures. These include the hexagonal wurtzite phases of $CuInS_2$, $CuInSe_2$, $Cu_2ZnSn(S_{1-x}Se_x)_4$, and Cu_2SnSe_3 nanocrystals. The discovery of crystal phases on the nanoscale that do not exist in their bulk analogues is a developing area of nanocrystal chemistry, and dichalcogenides are proving to be a useful synthetic tool in this regard.

The most recent application of dichalcogenide synthons for semiconductor nanocrystals is their use as precursors for surface ligands. While there is a rich history of using thiol ligands for semiconductor nanocrystals, the analogous selenol and tellurol ligands have not been studied, likely because of their oxidative instability. Dichalcogenides have proven useful in this regard, as they can be reduced *in situ* with diphenylphosphine to give the corresponding selenol or tellurol ligand that binds to the nanocrystal surface. This chemistry has been applied to the *in situ* synthesis and ligand binding of selenols to $PbSe$ nanocrystals and both selenols and tellurols to $CdSe$ nanocrystals. These initial studies have allowed the photophysics of these nanocrystal–ligand constructs to be investigated; in both cases, it appears that the selenol and tellurol ligands act as hole traps that quench the photoluminescence of the semiconductor nanocrystals.

1. INTRODUCTION

Colloidal semiconductor nanocrystals have been studied for >30 years because of their size-dependent optical and electronic properties. Solution-phase reactions to synthesize colloidal semiconductor nanocrystals are now achieving a high level of

control over the size, shape, size dispersion, and reproducibility of the resulting products. This level of synthetic control has

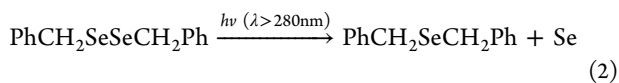
Received: August 3, 2015

Published: November 6, 2015

been brought forth by detailed studies into the mechanisms of precursor conversion,¹ a better understanding of impurities present in long-used solvents and ligands utilized in these syntheses,² and a continued interest in the development of new chemistries for colloidal semiconductor nanocrystal synthesis.^{3,4}

In 1993, Bawendi reported the synthesis of monodisperse nanocrystals of CdE (E = S, Se, Te) using a hot injection approach.⁵ Colloidal metal chalcogenide nanocrystals are usually synthesized by the solution-phase reaction between separate metal and chalcogenide precursors. While the metal precursor is now typically a simple metal carboxylate (rather than the organometallic precursors used in the early 1990s),⁶ a wide variety of different chalcogenide precursors have been employed over the past 30 years. Tertiary phosphine chalcogenides ($R_3P=E$, where R = alkyl or aryl and E = S, Se, or Te) are the most ubiquitous of precursors for the synthesis of metal chalcogenide nanocrystals⁵ and have been the traditional choice since the early work by Steigerwald that used them to prepare solid-state metal chalcogenides.⁷ These precursors are prepared by the oxidation of a tertiary phosphine with the elemental chalcogen to yield the phosphine chalcogenide.⁸ The ease of preparation coupled with their organic solubility are key factors that have made these precursors highly successful.⁶ Despite this success, there has been continued and longstanding interest in the exploration of alternate chalcogenide precursors. The various rationales behind exploring alternate precursors include precursor cost, ease of handling, toxicity, purity, and the ability to tune the nucleation and growth kinetics.⁹ Among the alternate chalcogenide precursors that have been most studied are sulfur and selenium dissolved in octadecene or amines,^{9–11} thio- and selenoureas,^{3,12} and silyl chalcogenides.^{5,13}

Diorganyl dichalcogenides ($R-E-E-R$, where E = S, Se, or Te and R = alkyl, allyl, benzyl, or aryl) are receiving renewed attention as highly versatile chalcogenide precursors for the synthesis of colloidal metal chalcogenide nanocrystals. Bell Laboratories utilized this type of chalcogenide precursor in the 1980s for the epitaxial growth of CdTe through the vapor-phase reaction between dimethyl ditelluride (Me_2Te_2) and Me_2Cd .¹⁴ It was found that in an organometallic vapor-phase epitaxial process, the ditelluride could be converted at lower temperatures than the monotelluride (i.e., Me_2Te). Earlier work by Chu and co-workers at Xerox Corporation in the 1970s showed that neat diselenides could be thermally or photolytically decomposed to give elemental selenium, monoselenide (R_2Se), and/or organic byproducts via radical scission of the Se–Se and Se–R bonds (eqs 1 and 2).^{15,16} Xerox's interest in



these molecules was rooted in their potential use as photoconductive elements in electrophotographic plates.¹⁷ Similarly, it was known that analogous ditelluride species can be photolyzed to yield a mixture of the monotelluride and elemental tellurium.^{18,19} Both S–S and C–S scission have also been demonstrated to occur during the photolysis of disulfides.²⁰ In each case, the radical species produced from the photolysis of the dichalcogenide can be intercepted by

tertiary phosphines to yield the corresponding phosphine chalcogenide.^{19,21–23}

In 2002, Schlecht and co-workers first utilized these chalcogenide precursors to synthesize metal chalcogenide nanoparticulates via the solution-phase reaction of activated Sn^0 nanoparticles with diphenyl diselenide (Ph_2Se_2) or diphenyl ditelluride (Ph_2Te_2) to yield $SnSe$ or $SnTe$, respectively.²⁴ Activated Sn^0 nanoparticles were reacted directly with Ph_2Te_2 in diglyme at 165 °C to yield $SnTe$ and Ph_2Te . The analogous reaction of activated Sn^0 nanoparticles with Ph_2Se_2 in diglyme at 165 °C yielded amorphous $SnSe$. While there was no demonstration of control over the morphology or crystallinity in the resulting nanoparticulates, this report served as the first example that dichalcogenides could be successfully utilized as synthons for nanoscale metal chalcogenides.

2. SYNTHONS FOR BINARY METAL CHALCOGENIDE NANOCRYSTALS

In 2009, we began to draw an analogy between the work of Schlecht and our research using dialkyl peroxides as oxygen transfer reagents for the synthesis of metal oxide nanocrystals. In our work, $In(acac)_3$ (acac = acetylacetone) was reacted with di-*tert*-butyl peroxide ($'Bu_2O_2$) using a “heating up” method in a mixture of oleylamine and lauric acid to yield 7 nm In_2O_3 nanocrystals at temperatures as low as 120 °C.²⁵ It was demonstrated that crystalline In_2O_3 does not nucleate under these conditions without the presence of the peroxide, suggesting that oxygen transfer to In^{3+} is made possible by decomposition of the peroxide precursor rather than the more common $In(acac)_3$ pyrolysis or hydrolysis pathways that operate at higher temperatures.²⁶ We posited that if peroxides could be used to transfer oxygen to Lewis acidic metal centers, then perhaps this chemistry could be expanded to the synthesis of metal chalcogenide nanocrystals using dichalcogenides such as those employed by Schlecht.

Indeed, the corresponding reaction between $In(acac)_3$ and di-*tert*-butyl disulfide ($'Bu_2S_2$) in oleylamine at 180 °C yielded crystalline β - In_2S_3 nanorods (Figure 1).²⁷ The resulting

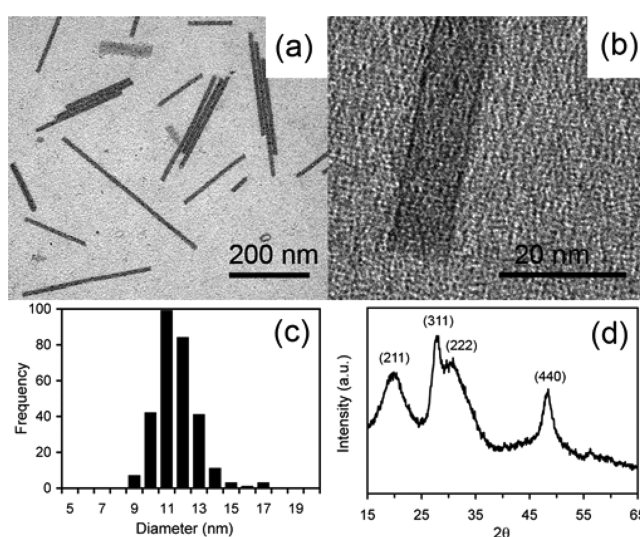


Figure 1. (a) Low- and (b) high-resolution transmission electron microscopy (TEM) images of In_2S_3 nanorods synthesized using $'Bu_2S_2$ as the sulfur source. (c) Size histogram of the nanorod diameters. (d) X-ray diffraction (XRD) pattern of the In_2S_3 nanorods. Adapted from ref 27. Copyright 2009 American Chemical Society.

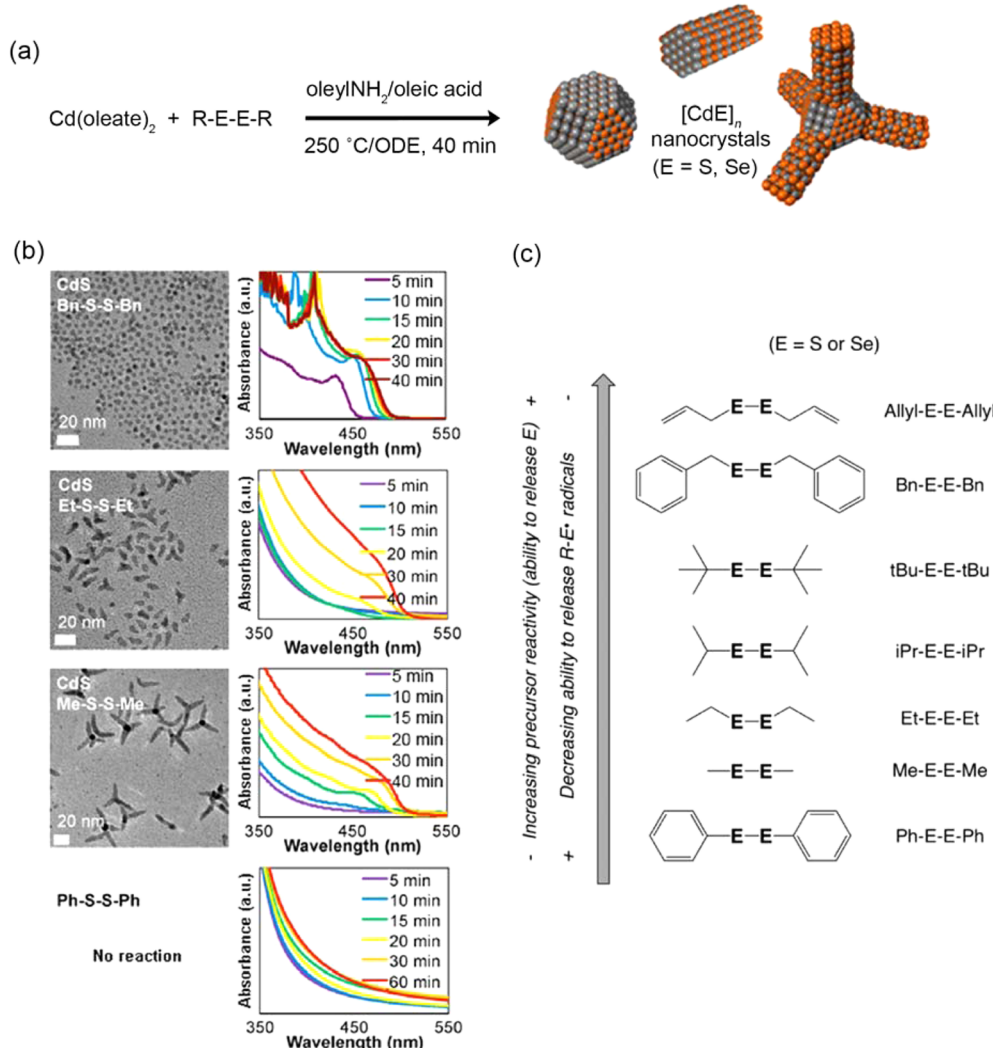


Figure 2. (a) Reaction scheme for the synthesis of CdE ($E = S, Se$) nanocrystals using dichalcogenide precursors. (b) Representative TEM images (left) and time evolution of the absorption spectra (right) of CdS quantum dots, nanorods, and tetrapods synthesized with dibenzyl, diethyl, and dimethyl disulfide precursors, respectively. Ph_2S_2 was unreactive under identical conditions. (c) Scheme showing that as the C–S or C–Se bond dissociation energy increases, the dichalcogenides become less reactive toward Cd(oleate)_2 under otherwise identical reaction conditions. Adapted from ref 35. Copyright 2013 American Chemical Society.

nanorods were polydisperse in length (mean length = 170 nm) with an average diameter of 11.5 ± 1.3 nm. It was determined that the $^t\text{Bu}_2\text{S}_2$ was key in the synthesis of the $\beta\text{-In}_2\text{S}_3$ nanorods. Using $^t\text{BuSH}$ as the sulfur source under otherwise identical conditions (and equivalents of sulfur atoms) yielded ill-defined zero-dimensional (0D) nanocrystals instead of nanorods, while elemental sulfur dissolved in oleylamine failed to produce any crystalline product at 180 °C. It is likely a combination of the amine and Lewis acidic metal that leads to decomposition of $^t\text{Bu}_2\text{S}_2$ and transfer of sulfur under these conditions.²⁸ The thermal decomposition of $^t\text{Bu}_2\text{S}_2$ begins at approximately 375 °C, which is well above the reaction temperature employed for the synthesis of the nanorods. Nockemann and co-workers later utilized Ph_2Se_2 to synthesize microcrystalline In_2Se_3 by reaction with chloroindate(III) ionic liquids at temperatures ranging from 200 to 280 °C.²⁹ While it is clear that the diselenide reacts with In^{3+} to form microcrystalline In_2Se_3 , the reaction in long-chain coordinating solvents to arrest the growth of In_2Se_3 nanocrystals has not yet been reported.

In an attempt to synthesize SnSe nanocrystals, di-*tert*-butyl diselenide ($^t\text{Bu}_2\text{Se}_2$) was reacted with a Sn^{2+} precursor (SnCl_2) in a mixture of dodecylamine and dodecanethiol at 180 °C.³⁰ When a stoichiometric amount of $^t\text{Bu}_2\text{Se}_2$ was used, orthorhombic SnSe nanocrystals resulted; however, when excess $^t\text{Bu}_2\text{Se}_2$ (i.e., 2 molar equiv of selenium relative to tin) was used, crystalline Berndtite SnSe_2 formed. The resulting SnSe nanocrystals were anisotropic with polydisperse lengths and widths of 19.0 ± 5.1 nm. This result stands in contrast to the original work of Schlecht, which resulted in amorphous SnSe nanoparticles after the reaction of an activated Sn^0 nanoparticle precursor with Ph_2Se_2 at 165 °C.²⁴ Here the reaction of a Sn^{2+} precursor with the proper stoichiometric amount of $^t\text{Bu}_2\text{Se}_2$ successfully yields SnSe nanocrystals at 180 °C.

In addition to these initial examples, dichalcogenides have also been successfully employed for the synthesis of many other binary metal chalcogenide nanocrystals with varying degrees of morphological control, including Cu_{2-x}S ,³¹ Cu_{2-x}Se ,³² ZnSe ,³³ GeSe ,³⁴ CdS ,³⁵ CdSe ,³⁶ MoSe_2 ,^{36,37} WSe_2 ,³⁶ and BiSe nanocrystals.³⁸ In an elegant study, Vela and co-workers investigated

how the dichalcogenide precursor reactivity can be used to tune the morphology of CdS and CdSe nanocrystals with a series of R_2E_2 precursors (R = allyl, benzyl, *tert*-butyl, isopropyl, ethyl, methyl, phenyl; E = S, Se).³⁵ When differently substituted disulfide precursors were injected into a solution of $Cd(\text{oleate})_2$ with oleic acid and oleylamine in 1-octadecene at 250 °C, it was observed that under otherwise identical conditions the precursors yielded differently shaped nanocrystals (Figure 2a). That is, dibenzyl disulfide (Bn_2S_2) yielded 0D CdS nanocrystals, diethyl disulfide (Et_2S_2) yielded 1D CdS nanorods, and dimethyl disulfide (Me_2S_2) yielded 3D tetrapods. It was also observed that diphenyl disulfide (Ph_2S_2) did not afford CdS nanocrystals at all (Figure 2b).

In order for the dichalcogenides to be converted into monomers that feed into the CdE nanocrystal nucleation event, both the C–E and E–E bonds in the precursor must break. Diallyl disulfide was calculated by density functional theory, using the Boese–Martin Kinetics functional, to have the lowest C–S bond dissociation energy (46 kcal/mol), followed by diethyl and dimethyl disulfide (58 and 59 kcal/mol, respectively) and Ph_2S_2 (70 kcal/mol). According to their calculations, the S–S bond dissociation energy is independent of the organic substituent for this series (i.e., on the order of 60 kcal/mol for R = allyl, Bn , ^tBu , ^iPr , Et, and Me), except for Ph_2S_2 , which has a lower S–S bond dissociation energy by ca. 15 kcal/mol. Vela and co-workers rationalized that the dichalcogenides with the weakest C–S bonds, such as $(\text{allyl})_2S_2$, are most reactive, leading to CdS clusters. Dichalcogenide precursors with stronger C–S bonds, such as Et_2S_2 and Me_2S_2 , react more slowly and selectively to yield anisotropic CdS nanocrystals such as nanorods and tetrapods, respectively. On the other hand, the Ph_2S_2 precursor possesses stronger C–S bonds and is unreactive in the sense that it does not lead to CdS nanocrystal formation; however, the relatively weak S–S bond may lead to homolytic bond scission to yield thiy radicals (Figure 2c).

Vela and co-workers hypothesized that the similar C–S and S–S bond dissociation energies in the diethyl and dimethyl disulfide precursors make S–S bond scission an equally thermodynamically probable event and that it may be the resulting thiyl radicals that influence the morphology of the nanocrystals. Indeed, utilizing the Ph_2S_2 precursor (which readily gives thiyl radicals as a result of its weak S–S bond) in 1:1 stoichiometry with precursors that yield only 0D quantum dots on their own (i.e., dibenzyl, di-*tert*-butyl, and diisopropyl disulfide) gives anisotropic CdS nanocrystals. Similar results were achieved with the analogous diselenides to give CdSe nanocrystals with controlled size and morphology depending on the organic substituent.

3. SYNTHONS FOR PHOTOCHEMICAL SYNTHESIS OF NANOCRYSTALS

Reactions that utilize low-temperature photochemical conversion of molecular precursors to controllably afford metal(loid), metal oxide, and metal chalcogenide nanocrystals are gaining in popularity.^{39,40} Along these lines, we demonstrated that well-defined Te nanorods could be prepared by the facile room-temperature photolysis of di-*tert*-butyl ditelluride ($^t\text{Bu}_2Te_2$) in an aqueous micellar system (Figure 3).⁴¹ As a consequence of the low bond dissociation energies of the Te–Te and C–Te bonds (36 and 47 kcal/mol, respectively),⁴² UV light is able to cause homolytic bond cleavage in $^t\text{Bu}_2Te_2$ resulting in the extrusion of elemental Te. Upon photolysis, the

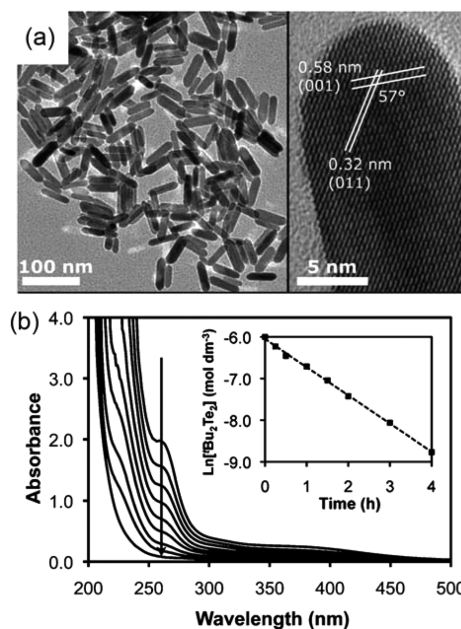


Figure 3. (a) TEM images of Te nanorods at low- (left) and high-resolution (right) prepared from the photolysis of $^t\text{Bu}_2\text{Te}_2$. (b) Temporal changes in the UV–vis spectrum of $^t\text{Bu}_2\text{Te}_2$ during the photolytic decomposition with 254 nm irradiation over 12 h. The apparent first-order reaction kinetics with respect to the ditelluride is plotted in the inset. Adapted with permission from ref 41. Copyright 2009 The Royal Society of Chemistry.

$^t\text{Bu}_2\text{Te}_2$ precursor was shown to decompose with first-order kinetics ($k = 0.68 \text{ h}^{-1}$). The resulting nanorods were single-crystalline tetragonal Te possessing an average diameter of $12.7 \pm 3.0 \text{ nm}$ and an average length of $46.5 \pm 9.4 \text{ nm}$ (aspect ratio = 3.7). Much in the same way that $^t\text{Bu}_2\text{Te}_2$ was shown to photolytically decompose to give Te nanorods, we found that $^t\text{Bu}_2\text{Se}_2$ is converted to amorphous red Se upon irradiation with 254 nm light in an aqueous micellar system.³⁸ When mixed in 1:2 stoichiometry with Ph_3Bi , $^t\text{Bu}_2\text{Se}_2$ is photolytically converted to sub-5 nm BiSe nanocrystals of the Nevesite phase.³⁸

4. SYNTHONS FOR COMPOSITIONALLY COMPLEX METAL CHALCOGENIDE NANOCRYSTALS

Among the most popular applications of dichalcogenide precursors has been their use in the synthesis of ternary and quaternary metal chalcogenide nanocrystals, often in metastable crystal phases. In 2009, we reported the synthesis of monodisperse CuInS_2 nanocrystals using $^t\text{Bu}_2\text{S}_2$ as the sulfur source.⁴³ Prior to this, CuInS_2 nanocrystals had been synthesized using dithiocarbamates,⁴⁴ thiols,⁴⁵ or elemental sulfur⁴⁶ at temperatures ranging from 180 to 250 °C. The majority of these syntheses yielded CuInS_2 nanocrystals in the thermodynamically preferred, tetragonal chalcopyrite phase. The reaction between CuCl , $\text{In}(\text{acac})_3$, and $^t\text{Bu}_2\text{S}_2$ in oleylamine and 1-dodecanethiol at 180 °C yielded monodisperse 7 nm CuInS_2 nanocrystals (Figure 4a). Interestingly, the resulting nanocrystals were found to exist in a metastable hexagonal wurtzite phase of CuInS_2 rather than the chalcopyrite phase (Figure 4b). In the bulk, wurtzite CuInS_2 is a high-temperature phase that is stable between 1045 and 1090 °C, in which the copper and indium cations randomly share common lattice positions.⁴⁷ The phase diagram of CuInS_2 shows a very

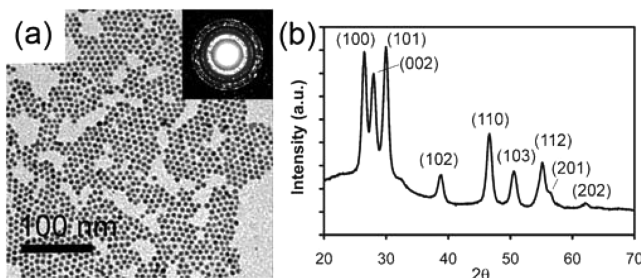


Figure 4. (a) TEM image of CuInS_2 nanocrystals synthesized using $^t\text{Bu}_2\text{S}_2$ as the sulfur source. (b) XRD pattern illustrating the wurtzite phase of the CuInS_2 nanocrystals. Adapted from ref 43. Copyright 2009 American Chemical Society.

narrow composition window for the thermodynamically preferred chalcopyrite phase, whereby the Cu:In ratio cannot deviate significantly from 1:1; however, for the wurtzite phase, the Cu:In ratio can vary over a wide composition range. This may be significant because the nanocrystals were found to nucleate in a very copper-rich ($\text{Cu:In} \approx 6:1$) wurtzite phase before becoming slightly less copper-rich ($\text{Cu:In} \approx 4.6:1$) upon size focusing to 7 nm nanocrystals. It was also found that under these conditions elemental sulfur dissolved in oleylamine did not give a crystalline product, while an equimolar amount (per sulfur atom) of $^t\text{BuSH}$ gave chalcopyrite CuInS_2 . Therefore, the decomposition and sulfur transfer rates of the disulfide appear to be different enough to exert a kinetic influence on the phase determination.

In much the same way, it was found that a metastable wurtzite phase of CuInSe_2 could be accessed using Ph_2Se_2 .⁴⁸ The reaction between CuCl , $\text{In}(\text{acac})_3$, and Ph_2Se_2 in oleylamine at 180 °C yielded polydisperse CuInSe_2 nanocrystals with a mean diameter of 30 nm. The diffraction data for the resulting nanocrystals did not match those for the expected chalcopyrite phase of CuInSe_2 ; however, a good match was achieved with a simulated wurtzite structure where Cu^+ and In^{3+} share a 50/50 occupancy probability on the cation lattice positions. Prior to this, the wurtzite phase for bulk CuInSe_2 was unknown. Again, it was found that specific reaction conditions were needed to achieve the metastable product. Using either selenium dissolved in oleylamine or selenourea as the selenium precursor resulted in the formation of chalcopyrite CuInSe_2 nanocrystals. As a follow-up to our initial report, Wang et al.⁴⁹ were able to achieve monodisperse 21 nm wurtzite CuInSe_2

nanocrystals by the analogous reaction of $\text{Cu}(\text{oleate})_2$, InCl_3 , and Ph_2Se_2 in oleylamine at 255 °C.

Wang and co-workers extended the utility of dichalcogenides to the synthesis of quaternary semiconductor nanocrystals. In their work, a mixture of $\text{Cu}(\text{oleate})_2$, $\text{Zn}(\text{oleate})_2$, $\text{Sn}(2\text{-ethylhexanoate})_2$, and Ph_2Se_2 was reacted in oleylamine at 255 °C to give 19 nm $\text{Cu}_2\text{ZnSnSe}_4$ nanocrystals.⁵⁰ Interestingly, the use of Ph_2Se_2 as the chalcogen precursor for multinary semiconductor nanocrystals again resulted in the formation of a wurtzite phase. Prior syntheses of $\text{Cu}_2\text{ZnSnSe}_4$ nanocrystals had resulted in the stannite or kesterite phase of this material.⁵¹ Wurtzite $\text{Cu}_2\text{ZnSnSe}_4$ is a metastable phase that is typically stable at high temperatures for the bulk material, whereas the stannite and kesterite phases are more thermodynamically stable. When Ph_2Se_2 was replaced with either elemental selenium or selenourea, the $\text{Cu}_2\text{ZnSnSe}_4$ nanocrystals were found to nucleate and grow in the stannite phase. Again, the kinetics of selenium transfer from the diselenide appears to be key in determining the phase in these multinary semiconductor nanocrystals. The groups of Yu and Ryan independently extended this synthesis to composition- and band-gap-tunable wurtzite $\text{Cu}_2\text{ZnSn}(\text{S}_{1-x}\text{Se}_x)_4$ nanocrystals, where controlled ratios of 1-dodecanethiol to Ph_2Se_2 were used to tune the S:Se ratio in the final nanocrystals.^{52,53} The band gaps of $\text{Cu}_2\text{ZnSn}(\text{S}_{1-x}\text{Se}_x)_4$ nanocrystals were tuned from about 1.5 to 1.0 eV for $x = 0$ to 1, respectively (Figure 5a), which is a wider energy range than can be compositionally accessed with the kesterite or stannite phases.⁵² In turn, the near-band-edge emission of these nanocrystals was also demonstrated to vary over a comparable energy range with composition (Figure 5b).

Yu and co-workers further expanded this method of synthesizing $\text{Cu}_2\text{ZnSn}(\text{S}_{1-x}\text{Se}_x)_4$ nanocrystals to linearly arranged zinc blende- and wurtzite-derived polytypic nanocrystals.⁵⁴ In this report, CuI , $\text{Zn}(\text{OAc})_2$, SnCl_2 , and 1-dodecanethiol were reacted with Ph_2Se_2 in oleylamine at different temperatures to produce polytypic nanocrystals. When nucleated at relatively low temperatures (220–240 °C), the nanocrystals adopt a wurtzite-derived structure. As the reaction temperature is ramped to higher temperatures postnucleation (i.e., 260–320 °C), increasingly larger fractions of zinc blende-derived $\text{Cu}_2\text{ZnSn}(\text{S}_{1-x}\text{Se}_x)_4$ nucleates and grows epitaxially from the wurtzite-type core. This is consistent with wurtzite $\text{Cu}_2\text{ZnSn}(\text{S}_{1-x}\text{Se}_x)_4$ being a metastable, kinetically accessed product under these particular reaction conditions and zinc

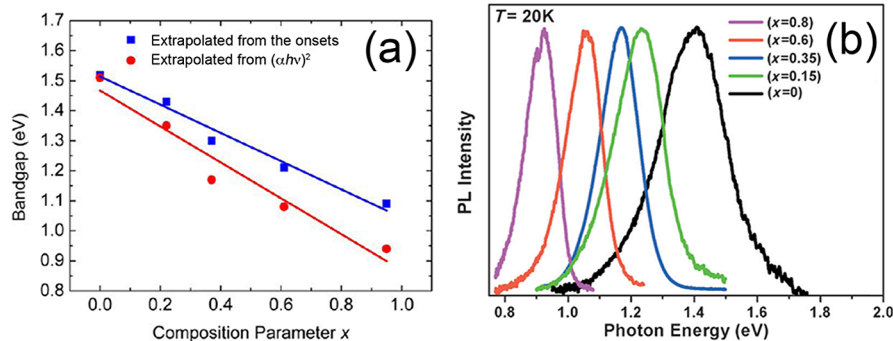


Figure 5. (a) Experimental band gaps of $\text{Cu}_2\text{ZnSn}(\text{S}_{1-x}\text{Se}_x)_4$ nanocrystals synthesized using Ph_2Se_2 as the selenium precursor. Adapted from ref 52. Copyright 2013 American Chemical Society. (b) Low-temperature photoluminescence emission of $\text{Cu}_2\text{ZnSn}(\text{S}_{1-x}\text{Se}_x)_4$ nanocrystals with varying x . Adapted with permission from ref 53. Copyright 2013 John Wiley and Sons.

blende-derived $\text{Cu}_2\text{ZnSn}(\text{S}_{1-x}\text{Se}_x)_4$ being the thermodynamically preferred phase at higher temperatures.

Diselenides have also been used to synthesize a series of other ternary, quaternary, and quinary metal chalcogenide nanocrystals, including $\text{Sn}_x\text{Ge}_{1-x}\text{Se}$,⁵⁵ $\text{Cu}_{2-x}\text{S}_y\text{Se}_{1-y}$,⁵⁶ $\text{Cu}_2\text{CdSn}(\text{S}_{1-x}\text{Se}_x)_4$,⁵⁷ CuFeSe_2 ,⁵⁸ and Cu_2SnSe_3 .^{59,60} In the first such report for Cu_2SnSe_3 nanocrystals, we reacted CuCl , SnI_4 , and ${}^t\text{Bu}_2\text{Se}_2$ in dodecylamine and 1-dodecanethiol at 180 °C to yield monodisperse, 15 nm Cu_2SnSe_3 nanocrystals.⁵⁹ As in other studies that utilized dichalcogenide precursors at relatively low reaction temperatures to synthesize compositionally complex metal chalcogenides, we found that the resulting nanocrystals adopt a metastable wurtzite structure that is not found in the bulk. The metastable wurtzite phase can be obtained instead of the thermodynamically preferred cubic phase through a combination of reaction parameters, such as ligand choice and chalcogenide precursor. In an extension of this work, Ryan and co-workers successfully synthesized Cu_2SnSe_3 tetrapods through high-temperature injection of Ph_2Se_2 followed by a lower-temperature growth stage.⁶⁰ In this way, they could successfully nucleate the thermodynamically preferred cubic polymorph and then grow metastable wurtzite arms off the cubic core to produce the tetrapod nanocrystal morphology (Figure 6).

5. SYNTHONS FOR NANOCRYSTAL LIGANDS

In addition to their ability to act as precursors for metal chalcogenide nanocrystal syntheses, dichalcogenides have more recently been employed as precursors for nanocrystal surface ligands. Beard and co-workers first utilized this approach to install alkylselenolate ligands on PbSe nanocrystals.⁶¹ An *in situ* reduction of dioctadecyl diselenide with diphenylphosphine was performed in the presence of PbSe nanocrystals capped with oleate ligands in hexanes. In this reduction, the diselenide reacts with diphenylphosphine to give a selenol and Ph_2PSeR .⁶² The resulting octadecylselenol reduction product undergoes proton exchange with the native oleate ligands to produce surface-bound selenolates, which induce nanocrystal flocculation from hexanes. The ligand exchange decreases the Pb:Se ratio in these Pb -rich nanocrystals and was shown by solution ^1H NMR spectroscopy to quantitatively displace the oleate ligands. Following ligand exchange, the octadecylselenolate-capped PbSe nanocrystals are more resistant to short-term oxidation (perhaps stemming from strong Pb-Se surface passivation) and possess a new dark hole trap that quenches the nanocrystal photoluminescence (Figure 7).

We extended the work of Beard et al. to the modular installation of a series of small chalcogenol ligands onto the surface of CdSe nanocrystals. In our work, *in situ* reduction of R_2E_2 ($\text{R} = {}^t\text{Bu}, \text{Bn}, \text{Ph}; \text{E} = \text{S}, \text{Se}, \text{Te}$) with diphenylphosphine was performed in the presence of CdSe nanocrystals capped with stearate ligands in toluene.⁶² Ligand exchange was evidenced by nanocrystal flocculation from the toluene suspension; however, ligand exchange was not found to be quantitative in this system (as probed by a combination of NMR and FT-IR spectroscopies and thermogravimetric analysis). For the diphenyl dichalcogenides as a model system, ligand exchange via *in situ* reduction of Ph_2S_2 , Ph_2Se_2 , and Ph_2Te_2 to yield the corresponding thiol, selenol, and telluro resulted in ~80, 70, and 80% removal of the stearate ligands, respectively. After exchange with the small chalcogenol ligands, the CdSe nanocrystals were readily dispersible in moderately polar solvents such as tetramethylurea and *N,N*-dimethylacet-

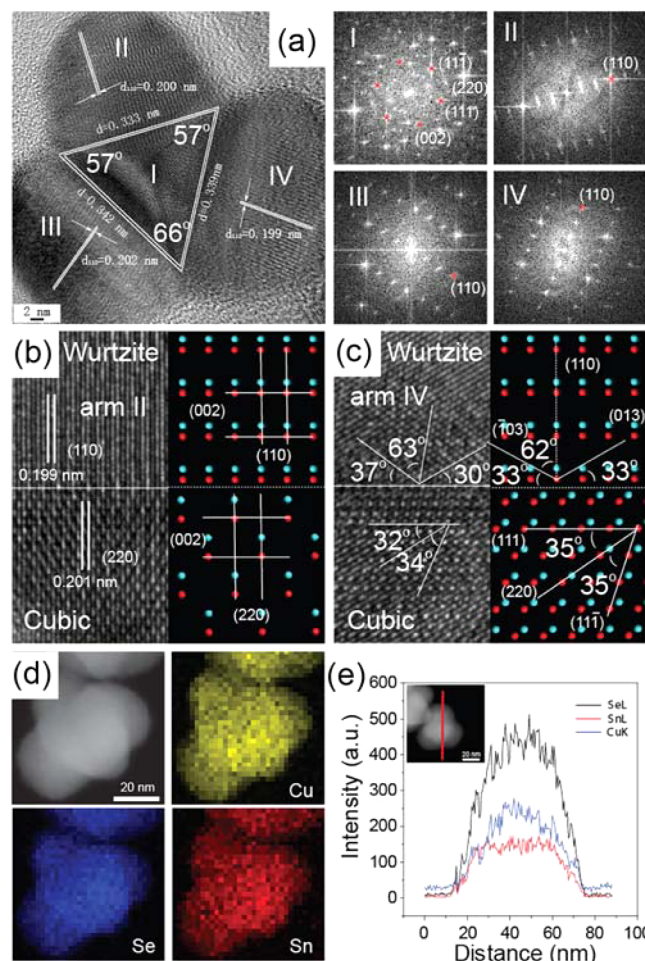


Figure 6. (a) High-resolution TEM image of a Cu_2SnSe_3 tetrapod synthesized using Ph_2Se_2 and the corresponding FFT patterns. (b) High-resolution TEM images of the interface between arm II and the core (left) and a crystal model of the interface (right). (c) High-resolution TEM images of the interface between arm IV and the core (left) and a crystal model of the interface (right). (d) Scanning TEM (STEM) image and energy-dispersive X-ray spectroscopy (EDS) elemental maps of a Cu_2SnSe_3 tetrapod. (e) EDS line scan of a Cu_2SnSe_3 tetrapod and (inset) the corresponding STEM image. Adapted from ref 60. Copyright 2013 American Chemical Society.

tamide to form stable colloidal suspensions. As with selenol binding to PbSe nanocrystals, time-resolved and low-temperature photoluminescence measurements demonstrated that the thiol (as widely known), selenol, and tellurol ligands all quench photoluminescence by hole trapping. It was found that the selenol and tellurol ligands possess a larger thermodynamic driving force for hole transfer than the thiol ligands, thus quenching the photoluminescence quantum yield more efficiently.

6. CONCLUSIONS AND OUTLOOK

Several dozen publications have now reported the use of dichalcogenide precursors for the synthesis of metal chalcogenide nanocrystals, many of which are compositionally complex materials. Dichalcogenides are thus proving to be a useful class of new precursors for the synthesis of metal chalcogenide nanocrystals. They represent a viable alternative to the better-studied phosphine chalcogenide, dissolved sulfur and selenium, thio- and selenourea, and silyl chalcogenide precursors. The

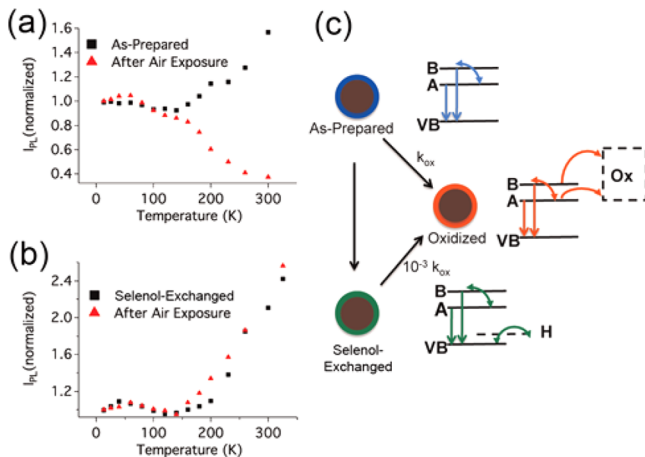


Figure 7. (a, b) Plots of integrated photoluminescence intensity vs temperature for (a) pristine as-prepared and air-exposed as-prepared PbSe nanocrystals and (b) selenol-exchanged and air-exposed selenol-exchanged PbSe nanocrystals. (c) Relaxation pathways for excited populations in as-prepared, selenol-exchanged, and oxidized PbSe nanocrystals. Solid lines represent bright states, while dashed lines represent dark states. The selenol-exchanged nanocrystals are more resistant to oxidation and also possess a dark hole-trap state. Adapted from ref 61. Copyright 2012 American Chemical Society.

apparent benefits of these precursors are fivefold: (i) they represent the first and only common precursor type that can function as chalcogen transfer reagents for each of the group VI elements (i.e., to make metal oxide, metal sulfide, metal selenide, and metal telluride nanocrystals); (ii) they possess relatively weak E–E bonds (roughly 50% the bond strength of the P=E bonds) that are cleaved at low reaction temperatures; (iii) the organic substituents can be tuned to affect the reactivity; (iv) they are soluble in organic solvents; and (v) many are commercially available. The general effectiveness and material scope allowed by these precursors represents a significant advancement. Indeed, a number of metastable and *previously unknown* crystal phases for certain bulk materials have been discovered for nanocrystals synthesized using these precursors. The discovery of crystal phases on the nanoscale that do not exist in the corresponding bulk materials is a still developing area of nanocrystal chemistry, and it appears that dichalcogenide precursors may be a useful synthetic tool in this regard.

Aside from the work by Vela,³⁵ there have been no mechanistic studies on nanocrystal chemistries utilizing dichalcogenides. In their study, they nicely demonstrated that the dichalcogenide C–E and E–E bond strengths affect the nanocrystal growth and resulting morphology. Further work is needed to understand how the dichalcogenide is converted in the presence of various ligands and metal precursors to give the chalcogenide monomer source needed for nucleation and growth. Early studies of the photolytic and thermolytic decomposition of diselenides and ditellurides suggest that these species decompose by bond homolysis to extrude elemental chalcogen;^{16,23} however, one might reasonably expect the molecular mechanism of precursor conversion to differ in the reaction gemish of nanocrystal syntheses. Elucidation of the dichalcogenide precursor conversion mechanism may help achieve more monodisperse nanocrystal ensembles, which is another outstanding challenge for many of the reported nanocrystal syntheses utilizing dichalcogenides.

Finally, dichalcogenides have more recently been applied as precursors for the *in situ* generation of thiol, selenol, and tellurol ligands for PbSe and CdSe nanocrystals. Selenol and tellurol species are prone to oxidative instability, so accessing them by *in situ* reduction with diphenylphosphine has allowed them to be studied as ligands for metal selenide nanocrystals. These initial investigations of selenol binding to PbSe nanocrystals as well as selenol and tellurol binding to CdSe nanocrystals suggest that chalcogenol ligands act as effective dark hole traps that quench the nanocrystal photoluminescence while increasing the oxidative stability of the nanocrystal core. Further work is needed to understand how these ligands affect the electronic structure and photophysics of other common semiconductor nanocrystals. A systematic computational study of chalcogenol binding to such semiconductor nanocrystals would be a useful predictive guide in these efforts.

■ AUTHOR INFORMATION

Corresponding Author

*E-mail: brutchey@usc.edu.

Notes

The authors declare no competing financial interest.

Biography

Richard L. Brutchey received his Ph.D. degree from the University of California, Berkeley, under the direction of T. Don Tilley and was a postdoctoral fellow with Daniel Morse at the University of California, Santa Barbara. He is currently an Associate Professor in the Department of Chemistry at the University of Southern California. His research focuses on the synthesis of inorganic materials and their application to sustainable energy solutions. More information about the Brutchey group can be found at <http://twitter.com/brutcheygroup>.

■ ACKNOWLEDGMENTS

The author acknowledges financial support from the National Science Foundation under DMR-1506189. He also thanks those co-workers that carried out much of the work described in this Account: Dr. P. Antunez, Dr. J. Buckley, Dr. E. Couderc, Dr. M. Franzman, Dr. M. Greaney, H. Hinton, Dr. M. Norako, V. Pérez, and Dr. D. Webber.

■ REFERENCES

- (1) Liu, H. T.; Owen, J. S.; Alivisatos, A. P. Mechanistic Study of Precursor Evolution in Colloidal Group II-VI Semiconductor Nanocrystal Synthesis. *J. Am. Chem. Soc.* **2007**, *129*, 305–312.
- (2) Wang, F.; Tang, R.; Buhro, W. E. The Trouble with TOPO; Identification of Adventitious Impurities Beneficial to the Growth of Cadmium Selenide Quantum Dots, Rods and Wires. *Nano Lett.* **2008**, *8*, 3521–3524.
- (3) Hendricks, M. P.; Campos, M. P.; Cleveland, G. T.; Jen-La Plante, I.; Owen, J. S. A Tunable Library of Substituted Thiourea Precursors to Metal Sulfide Nanocrystals. *Science* **2015**, *348*, 1226–1230.
- (4) Flamee, S.; Cirillo, M.; Abe, S.; De Nolf, K.; Gomes, R.; Aubert, T.; Hens, Z. Fast, High Yield, and High Solid Loading Synthesis of Metal Selenide Nanocrystals. *Chem. Mater.* **2013**, *25*, 2476–2483.
- (5) Murray, C. B.; Norris, D. J.; Bawendi, M. G. Synthesis and Characterization of Nearly Monodisperse CdE (E = Sulfur, Selenium, Tellurium) Semiconductor Nanocrystallites. *J. Am. Chem. Soc.* **1993**, *115*, 8706–8715.
- (6) Qu, L.; Peng, Z. A.; Peng, X. Alternative Routes to High Quality CdSe Nanocrystals. *Nano Lett.* **2001**, *1*, 333–337.

- (7) Stuczynski, S. M.; Kwon, Y.-U.; Steigerwald, M. L. The Use of Phosphine Chalcogenides in the Preparation of Cobalt Chalcogenides. *J. Organomet. Chem.* **1993**, *449*, 167–172.
- (8) Zingaro, R. A.; McGlothin, R. E. Some Phosphines, Phosphine Sulfides, and Phosphine Selenides. *J. Chem. Eng. Data* **1963**, *8*, 226–229.
- (9) Bullen, C.; van Embden, J.; Jasieniak, J.; Cosgriff, J. E.; Mulder, R. J.; Rizzato, E.; Gu, M.; Raston, C. L. High Activity Phosphine-Free Selenium Precursor Solution for Semiconductor Nanocrystal Growth. *Chem. Mater.* **2010**, *22*, 4135–4143.
- (10) Thomson, J. W.; Nagashima, K.; Macdonald, P. M.; Ozin, G. A. From Sulfur-Amine Solutions to Metal Sulfide Nanocrystals: Peering into the Oleylamine-Sulfur Black Box. *J. Am. Chem. Soc.* **2011**, *133*, 5036–5041.
- (11) Yu, W. W.; Peng, X. Formation of High-Quality CdS and Other II-VI Semiconductor Nanocrystals in Noncoordinating Solvents: Tunable Reactivity of Monomers. *Angew. Chem., Int. Ed.* **2002**, *41*, 2368–2371.
- (12) Liu, Y.-H.; Wayman, V. L.; Gibbons, P. C.; Loomis, R. A.; Buhro, W. E. Origin of High Photoluminescence Efficiencies in CdSe Quantum Belts. *Nano Lett.* **2010**, *10*, 352–357.
- (13) Hines, M. A.; Scholes, G. D. Colloidal PbS Nanocrystals with Size-Tunable Near-Infrared Emission: Observation of Post-Synthesis Self-Narrowing of Particle Size Distribution. *Adv. Mater.* **2003**, *15*, 1844–1849.
- (14) Kisker, D. W.; Steigerwald, M. L.; Kometani, T. Y.; Jeffers, K. S. Low Temperature Organometallic Vapor Phase Epitaxial Growth of CdTe using a New Organotellurium Source. *Appl. Phys. Lett.* **1987**, *50*, 1681–1683.
- (15) Chu, J. Y. C.; Lewicki, J. W. Thermal Decomposition of Bis(diphenylmethyl) Diselenide. *J. Org. Chem.* **1977**, *42*, 2491–2493.
- (16) Chu, J. Y. C.; Marsh, D. G.; Günther, W. H. H. Photochemistry of Organochalcogen Compounds. I. Photolysis of Benzyl Diselenide. *J. Am. Chem. Soc.* **1975**, *97*, 4905–4908.
- (17) Marsh, D. G. Microimaging Film Containing an Organic Diselenide, a Tertiary Phosphine or Phosphite and an Azo Organic Peroxide and the Use Thereof. U.S. Patent 4,106,936, August 5, 1978.
- (18) Spencer, H. K.; Cava, M. P. Organotellurium Chemistry. 2. Dibenzyl Ditelluride: Some Transformations Involving Loss of Tellurium. *J. Org. Chem.* **1977**, *42*, 2937–2939.
- (19) Brown, D. H.; Cross, R. J.; Millington, D. Photolysis of Diorganoditellurides in the Presence of Tertiary Phosphines. *J. Organomet. Chem.* **1977**, *125*, 219–223.
- (20) Byers, G. W.; Gruen, H.; Giles, H. G.; Schott, H. N.; Kampmeier, J. A. Photochemistry of Disulfides. I. Carbon-Sulfur Cleavage in the Photosensitized Decomposition of Simple Disulfides. *J. Am. Chem. Soc.* **1972**, *94*, 1016–1018.
- (21) Cross, R. J.; Millington, D. Selenium Abstraction from Diethyl Diselenide by Tertiary Phosphines. *J. Chem. Soc., Chem. Commun.* **1975**, 455–456.
- (22) Walling, C.; Rabinowitz, R. The Reaction of Trialkyl Phosphites with Thiyil and Alkoxy Radicals. *J. Am. Chem. Soc.* **1959**, *81*, 1243–1249.
- (23) Martens, J.; Praefcke, K. Photochemistry of Organic Selenium and Tellurium Compounds. *J. Organomet. Chem.* **1980**, *198*, 321–351.
- (24) Schlecht, S.; Budde, M.; Kienle, L. Nanocrystalline Tin as a Preparative Tool: Synthesis of Unprotected Nanoparticles of SnTe and SnSe and a New Route to $(\text{PhSe})_4\text{Sn}$. *Inorg. Chem.* **2002**, *41*, 6001–6005.
- (25) Franzman, M. A.; Pérez, V.; Brutchey, R. L. Peroxide-Mediated Synthesis of Indium Oxide Nanocrystals at Low Temperatures. *J. Phys. Chem. C* **2009**, *113*, 630–636.
- (26) Narayanaswamy, A.; Xu, H.; Pradhan, N.; Kim, M.; Peng, X. Formation of Nearly Monodisperse In_2O_3 Nanodots and Oriented Attached Nanoflowers: Hydrolysis and Alcoholysis vs Pyrolysis. *J. Am. Chem. Soc.* **2006**, *128*, 10310–10319.
- (27) Franzman, M. A.; Brutchey, R. L. Synthesis and Characterization of Indium Sulfide Nanorods. *Chem. Mater.* **2009**, *21*, 1790–1792.
- (28) Mori, K.; Nakamura, Y. Reaction of Sulfur Compounds Activated by Amines. II. Reaction of Sulfur and Some Aliphatic Primary Amines. *J. Org. Chem.* **1971**, *36*, 3041–3042.
- (29) Tyrrell, S.; Swadzba-Kwasny, M.; Nockemann, P. Ionothermal, Microwave-Assisted Synthesis of Indium(III) Selenide. *J. Mater. Chem. A* **2014**, *2*, 2616–2622.
- (30) Franzman, M. A.; Schlenker, C. W.; Thompson, M. E.; Brutchey, R. L. Solution-Phase Synthesis of SnSe Nanocrystals for Use in Solar Cells. *J. Am. Chem. Soc.* **2010**, *132*, 4060–4061.
- (31) Li, W.; Shavel, A.; Guzman, R.; Rubio-Garcia, J.; Flox, C.; Fan, J.; Cadavid, D.; Ibanez, M.; Arbiol, J.; Morante, J. R.; Cabot, A. Morphology Evolution of Cu_{2-x}S Nanoparticles: From Spheres to Dodecahedrons. *Chem. Commun.* **2011**, *47*, 10332–10334.
- (32) Wang, W.; Zhang, L.; Chen, G.; Jiang, J.; Ding, T.; Zuo, J.; Yang, Q. Cu_{2-x}Se Nanoctahedra: Controllable Synthesis and Optoelectronic Properties. *CrystEngComm* **2015**, *17*, 1975–1981.
- (33) Tyrrell, S.; Behrendt, G.; Liu, Y.; Nockemann, P. Zinc Selenide Nano- and Microspheres via Microwave-Assisted Ionothermal Synthesis. *RSC Adv.* **2014**, *4*, 36110–36116.
- (34) Xue, D.-J.; Tan, J.; Hu, J.-S.; Hu, W.; Guo, Y.-G.; Wan, L.-J. Anisotropic Photoresponse Properties of Single Micrometer-Sized GeSe Nanosheets. *Adv. Mater.* **2012**, *24*, 4528–4533.
- (35) Guo, Y.; Alvarado, S. R.; Barclay, J. D.; Vela, J. Shape-Programmed Nanofabrication: Understanding the Reactivity of Dichalcogenide Precursors. *ACS Nano* **2013**, *7*, 3616–3626.
- (36) Jung, W.; Lee, S.; Yoo, D.; Jeong, S.; Miro, P.; Kuc, A.; Heine, T.; Cheon, J. Colloidal Synthesis of Single-Layer MSe_2 ($\text{M} = \text{Mo}, \text{W}$) Nanosheets via Anisotropic Solution-Phase Growth Approach. *J. Am. Chem. Soc.* **2015**, *137*, 7266–7269.
- (37) Antunez, P. D.; Webber, D. H.; Brutchey, R. L. Solution-Phase Synthesis of Highly Conductive Tungsten Diselenide Nanosheets. *Chem. Mater.* **2013**, *25*, 2385–2387.
- (38) Webber, D. H.; Brutchey, R. L. Photochemical Synthesis of Bismuth Selenide Nanocrystals in an Aqueous Micellar Solution. *Inorg. Chem.* **2011**, *50*, 723–725.
- (39) Luz, A.; Malek-Luz, A.; Feldmann, C. Photochemical Synthesis of Particulate Main-Group Elements and Compounds. *Chem. Mater.* **2013**, *25*, 202–209.
- (40) Alvarado, S. R.; Guo, Y.; Ruberu, T. P. A.; Bakac, A.; Vela, J. Photochemical versus Thermal Synthesis of Cobalt Oxyhydroxide Nanocrystals. *J. Phys. Chem. C* **2012**, *116*, 10382–10389.
- (41) Webber, D. H.; Brutchey, R. L. Photolytic Preparation of Tellurium Nanorods. *Chem. Commun.* **2009**, 5701–5703.
- (42) Tel'noy, V. I.; Sheiman, M. S. Thermodynamics of Organoselenium and Organotellurium Compounds. *Russ. Chem. Rev.* **1995**, *64*, 309–316.
- (43) Norako, M. E.; Franzman, M. A.; Brutchey, R. L. Growth Kinetics of Monodisperse Cu-In-S Nanocrystals Using a Dialkyl Disulfide Sulfur Source. *Chem. Mater.* **2009**, *21*, 4299–4304.
- (44) Pan, D.; Wang, X.; Zhou, Z. H.; Chen, W.; Xu, C.; Lu, Y. Synthesis of Quaternary Semiconductor Nanocrystals with Tunable Band Gaps. *Chem. Mater.* **2009**, *21*, 2489–2493.
- (45) Zhong, H.; Zhou, Y.; Ye, M.; He, Y.; Ye, J.; He, C.; Yang, C.; Li, Y. Controlled Synthesis and Optical Properties of Colloidal Ternary Chalcogenide CuInS_2 Nanocrystals. *Chem. Mater.* **2008**, *20*, 6434–6443.
- (46) Panthani, M. G.; Akhavan, V.; Goodfellow, B.; Schmidtke, J. P.; Dunn, L.; Dodabalapur, A.; Barbara, P. F.; Korgel, B. A. Synthesis of CuInS_2 , CuInSe_2 , and $\text{Cu}(\text{In}_{x}\text{Ga}_{1-x})\text{Se}_2$ (CIGS) Nanocrystal "Inks" for Printable Photovoltaics. *J. Am. Chem. Soc.* **2008**, *130*, 16770–16777.
- (47) Binsma, J. J. M.; Giling, L. J.; Bloem, J. Phase Relations in the System $\text{Cu}_2\text{S}-\text{In}_2\text{S}_3$. *J. Cryst. Growth* **1980**, *50*, 429–436.
- (48) Norako, M. E.; Brutchey, R. L. Synthesis of Metastable Wurtzite CuInSe_2 Nanocrystals. *Chem. Mater.* **2010**, *22*, 1613–1615.
- (49) Wang, J.-J.; Wang, Y.-Q.; Cao, F.-F.; Guo, Y.-G.; Wan, L.-J. Synthesis of Monodispersed Wurtzite Structure CuInSe_2 Nanocrystals and Their Application in High-Performance Organic-Inorganic Hybrid Photodetectors. *J. Am. Chem. Soc.* **2010**, *132*, 12218–12221.

- (50) Wang, J.-J.; Hu, J.-S.; Guo, Y.-G.; Wan, L.-J. Wurtzite Cu₂ZnSnSe₄ Nanocrystals for High-Performance Organic-Inorganic Hybrid Photodetectors. *NPG Asia Mater.* **2012**, *4*, e2.
- (51) Shavel, A.; Arbiol, J.; Cabot, A. A Synthesis of Quaternary Chalcogenide Nanocrystals: Stannite Cu₂Zn_xSn_ySe_{1+x+2y}. *J. Am. Chem. Soc.* **2010**, *132*, 4514–4515.
- (52) Fan, F.-J.; Wu, L.; Gong, M.; Liu, G.; Wang, Y.-X.; Yu, S.-H.; Chen, S.; Wang, L.-W.; Gong, X.-G. Composition- and Band-Gap-Tunable Synthesis of Wurtzite-Derived Cu₂ZnSn(S_{1-x}Se_x)₄ Nanocrystals: Theoretical and Experimental Insights. *ACS Nano* **2013**, *7*, 1454–1463.
- (53) Singh, A.; Singh, S.; Levchenko, S.; Unold, T.; Laffir, F.; Ryan, K. M. Compositionally Tunable Photoluminescence Emission in Cu₂ZnSn(S_{1-x}Se_x)₄ Nanocrystals. *Angew. Chem., Int. Ed.* **2013**, *52*, 9120–9124.
- (54) Fan, F.-J.; Wu, L.; Gong, M.; Chen, S. Y.; Liu, G. Y.; Yao, H.-B.; Liang, H.-W.; Wang, Y.-X.; Yu, S.-H. Linearly Arranged Polytypic CZTSSe Nanocrystals. *Sci. Rep.* **2012**, *2*, 952.
- (55) Buckley, J. J.; Rabuffetti, F. A.; Hinton, H. L.; Brutchey, R. L. Synthesis and Characterization of Ternary Sn_xGe_{1-x}Se Nanocrystals. *Chem. Mater.* **2012**, *24*, 3514–3516.
- (56) Wang, J.-J.; Xue, D.-J.; Guo, Y.-G.; Hu, J.-S.; Wan, L.-J. Bandgap Engineering of Monodispersed Cu_{2-x}S_ySe_{1-y} Nanocrystals through Chalcogen Ratio and Crystal Structure. *J. Am. Chem. Soc.* **2011**, *133*, 18558–18561.
- (57) Wu, L.; Fan, F.-J.; Gong, M.; Ge, J.; Yu, S.-H. Selective Epitaxial Growth of Zinc Blende-Derivative on Wurtzite-Derivative: The Case of Polytypic Cu₂CdSn(S_{1-x}Se_x)₄ Nanocrystals. *Nanoscale* **2014**, *6*, 3418–3422.
- (58) Wang, W.; Jiang, J.; Ding, T.; Wang, C.; Zuo, J.; Yang, Q. Alternative Synthesis of CuFeSe₂ Nanocrystals with Magnetic and Photoelectric Properties. *ACS Appl. Mater. Interfaces* **2015**, *7*, 2235–2241.
- (59) Norako, M. E.; Greaney, M. J.; Brutchey, R. L. Synthesis and Characterization of Wurtzite Phase Copper Tin Selenide Nanocrystals. *J. Am. Chem. Soc.* **2012**, *134*, 23–26.
- (60) Wang, J.; Singh, A.; Liu, P.; Singh, S.; Coughlan, C.; Guo, Y.; Ryan, K. M. Colloidal Synthesis of Cu₂SnSe₃ Tetrapod Nanocrystals. *J. Am. Chem. Soc.* **2013**, *135*, 7835–7838.
- (61) Hughes, B. K.; Ruddy, D. A.; Blackburn, J. L.; Smith, D. K.; Bergren, M. R.; Nozik, A. J.; Johnson, J. C.; Beard, M. C. Control of PbSe Quantum Dot Surface Chemistry and Photophysics Using an Alkylselenide Ligand. *ACS Nano* **2012**, *6*, 5498–5506.
- (62) Buckley, J. J.; Couderc, E.; Greaney, M. J.; Munteanu, J.; Riche, C. T.; Bradforth, S. E.; Brutchey, R. L. Chalcogenol Ligand Toolbox for CdSe Nanocrystals and Their Influence on Exciton Relaxation Pathways. *ACS Nano* **2014**, *8*, 2512–2521.